

# Computer-Assisted Comparison of the Structural and Electronic Dispositions of Ebastine and Terfenadine

Victor Segarra, Manuel López, Hamish Ryder, José Maria Palacios and David J. Roberts

Research Centre, Almirall Prodesfarma, Barcelona, Spain

## Abstract

**Objective:** Ebastine and terfenadine are both marketed nonsedating H<sub>1</sub> histamine receptor antagonists. Although apparently similar in chemical structure, the compounds have different pharmacological profiles, particularly with respect to cardiac effects. These effects are consistently observed in a wide range of experimental models with terfenadine, but not with ebastine, despite the fact that the latter is more potent as an antihistamine. The objective of this study was to provide a structural basis to explain such differences.

**Design:** A complete computer-assisted conformational and electronic characterisation was made for both drugs.

**Results:** The preferred 3-dimensional spatial orientations were found to be different, as were the molecular locations of the highest occupied and lowest unoccupied molecular orbitals. Furthermore, for terfenadine, additional points of interaction as a hydrogen bond donor were found, which were not evident in ebastine or other noncardiotoxic antihistamines. These extra points of interaction were also found in other compounds that have shown cardiac effects similar to those of terfenadine.

Ebastine is a relatively new histamine H<sub>1</sub> receptor antagonist; it has been conceptually described<sup>[1]</sup> as a hybrid between the potent but sedative first generation antihistamine diphenylpyridine and the less potent, but nonsedative, second generation antihistamine terfenadine (fig. 1).

The validity of such a concept is supported by extensive pharmacological studies and clinical experience showing that, although ebastine is clearly a very potent and selective H<sub>1</sub> antihistamine, it penetrates the blood-brain barrier poorly and is accordingly devoid of sedative activity, even at doses several times higher than the recommended therapeutic dose of 10 mg/day.<sup>[2]</sup> Ebastine and terfenadine therefore inevitably share some common structural features: for example, the presence of two

aromatic rings and a protonatable nitrogen, which as previously reported are involved in the binding to histamine H<sub>1</sub> receptors;<sup>[3-5]</sup> and terminal tertiary butyl groups, which give rise to the respective pharmacologically active carboxylic acid metabolites, carebastine and fexofenadine, on oxidation.<sup>[6,7]</sup> Nevertheless, ebastine is clearly more potent than terfenadine as an H<sub>1</sub> receptor antagonist both *in vitro* and *in vivo*,<sup>[8,9]</sup> as well as in clinical practice (usual daily doses are 10mg and 120mg, respectively).

In clinical use, terfenadine, especially when coadministered with drugs such as ketoconazole and erythromycin, which inhibit its metabolism to fexofenadine, has occasionally been associated with prolongation of the cardiac QTc interval,

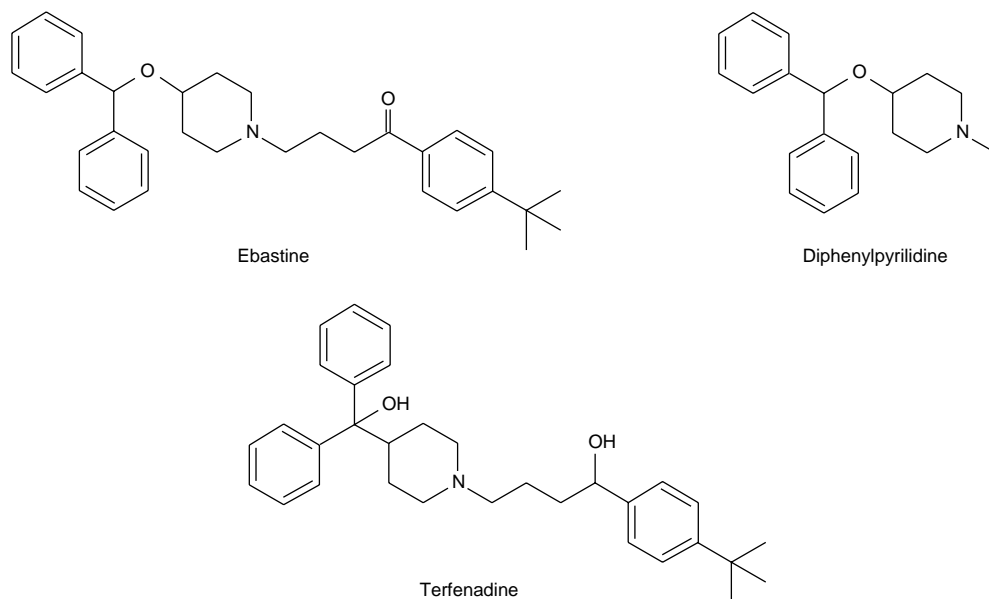


Fig. 1. Chemical structure of ebastine, terfenadine and diphenylpyrilidine.

altered T waves and induction of torsade de pointes, a normally self-limiting, but sometimes fatal, ventricular arrhythmia.<sup>[10]</sup> These cardiotoxic effects have been attributed to the ability of terfenadine to block cardiac potassium channels.<sup>[11,12]</sup>

The presence of some structural features common to ebastine and terfenadine, such as two phenyl rings and a basic nitrogen, which become visually exaggerated in simple 2-dimensional representations of chemical structure where subtle differences in both nucleus and side-chain are obscured, has raised questions concerning possible cardiotoxic effects of ebastine. Appropriate preclinical and clinical studies addressing this issue have shown very satisfactory results. Thus, although terfenadine at a concentration of 0.03  $\mu\text{mol/L}$  prolonged guinea-pig cardiac action potentials, ebastine, even at 3  $\mu\text{mol/L}$ , was without effect.<sup>[13]</sup> Similarly, terfenadine has been found to block  $\text{IC}_{50}$  (concentration producing 50% inhibition) 0.88  $\mu\text{mol/L}$  the delayed rectifier  $\text{K}^+$  current  $\text{Kv}1.5$ , cloned from hu-

man heart,<sup>[14]</sup> whereas ebastine has little effect in this model, even at 3  $\mu\text{mol/L}$ .<sup>[15]</sup> Similarly, *in vivo* studies have shown that, when infused directly into the coronary circulation of the anaesthetised dog, ebastine, unlike terfenadine, has no effect on the QTc interval.<sup>[16]</sup> Although some prolongation of the QTc interval was found in a conscious guinea-pig model following intravenous administration of ebastine, the doses used were high, being at least one order of magnitude greater than the terfenadine doses that produced similar effects.<sup>[17,18]</sup> Also, it has now been clearly demonstrated that the prolongation of the QTc interval in the same model after oral administration of ebastine in the presence of ketoconazole<sup>[19]</sup> is entirely due to the cardiac effects of ketoconazole.<sup>[18,20,21]</sup> Extensive evaluation of many thousand ECG traces obtained during clinical trials with ebastine has confirmed these preclinical data. In contrast to terfenadine, ebastine did not produce any morphological changes in the T wave or clinically meaningful prolongation of

the QTc interval, even in repeated doses of 100mg daily (10 times the usual recommended therapeutic dose), or when coadministered with ketoconazole or erythromycin.<sup>[2]</sup> Thus, the apparent, albeit superficial, 2-dimensional similarity between ebastine and terfenadine in chemical structure contrasts with their different pharmacological/toxicological and clinical profiles. We have compared the 3-dimensional structural and electronic features of these compounds, in search of possible differences to help explain the increased histamine H<sub>1</sub> receptor-antagonist activity and diminished cardiotoxicity of ebastine compared with terfenadine.

## Materials and Methods

The fully extended conformations of terfenadine and ebastine used as the starting point were constructed with standard bond lengths and angles by means of the Chem-X molecular modelling package. Energy minimisations and molecular dynamics simulations were performed by the full molecular mechanics force field implemented in Chem-X.<sup>[22,23]</sup>

The following molecular dynamics protocol was used to sample the conformational spaces for the protonated forms of both compounds (fig. 2). An infinite cut-off for the non-bonding interactions and a constant dielectric function ( $\xi = 80$ ) were employed throughout the procedure. The starting coordinates were minimised by using 100 steps of the steepest descents method followed by a conjugate gradient method (Fletcher-Reeves modification of the Polak-Ribière approach)<sup>[22]</sup> until convergence, which was reached with a  $1.0 \times 10^{-7}$  kcal • mol<sup>-1</sup> energy difference.

At this point, classical molecular dynamics,<sup>[24]</sup> which involved heating the molecule to 1000°K, was used for the conformational search. After equilibration, a 100 psec trajectory, with a step length of 0.005 psec, was simulated. 100 conformations separated by 1 psec were selected, and each one was subjected to extensive conjugate gradient energy minimisation until the root-mean-square gradient was less than 0.001 kcal • mol<sup>-1</sup> Å<sup>-1</sup>. After energy optimisation employing the whole set, the statistical

SAS package was used to perform a cluster graph analysis<sup>[25,26]</sup> of the resulting root-mean-square deviations for each pair of conformers in order to explore the whole cartesian space.<sup>[27]</sup> The 10 lower potential energy structures, together with another 20 structures obtained by extracting one set of coordinates every 5 psec from the trajectory, were selected as representatives of the whole conformational space. After superimposition analysis, the most abundant and stable conformations were identified and subsequently relaxed following another molecular dynamics protocol. Thus, the new coordinate sets were made at 310°K, with a step length of 0.005 psec during a 20 psec trajectory. The whole set was again minimised and, after cluster analysis, the lower potential energy structures were optimised by means of the AM1 Hamiltonian included in the Molecular Orbital PACKage (MOPAC)<sup>[28]</sup> to a gradient norm of less than 0.01 kcal • mol<sup>-1</sup>.<sup>[29]</sup>

The semi-empirical molecular orbital AM1 method, as implemented in the MOPAC program, was used to obtain the quantum mechanical molecular electrostatic potential (MEP)<sup>[30]</sup> and the frontier orbitals [the highest occupied molecular orbital (HOMO) and the lowest unoccupied molecular orbital (LUMO)]. The physicochemical properties were analysed by means of GRID<sup>[31-35]</sup> computations. This program determines the attraction of molecules for different chemical probes. Favourable areas of interaction were displayed as contours in 3-dimensional space.

## Results

### Conformational Analysis by Use of a Molecular Dynamics Procedure

Both terfenadine and ebastine have a large number of rotatable bonds that make it difficult to explore the conformational space by means of systematic conformational analysis. Because of its efficiency in crossing energy barriers in multidimensional conformational space, a high temperature molecular dynamics method was chosen to explore all the conformational space.<sup>[24]</sup> The

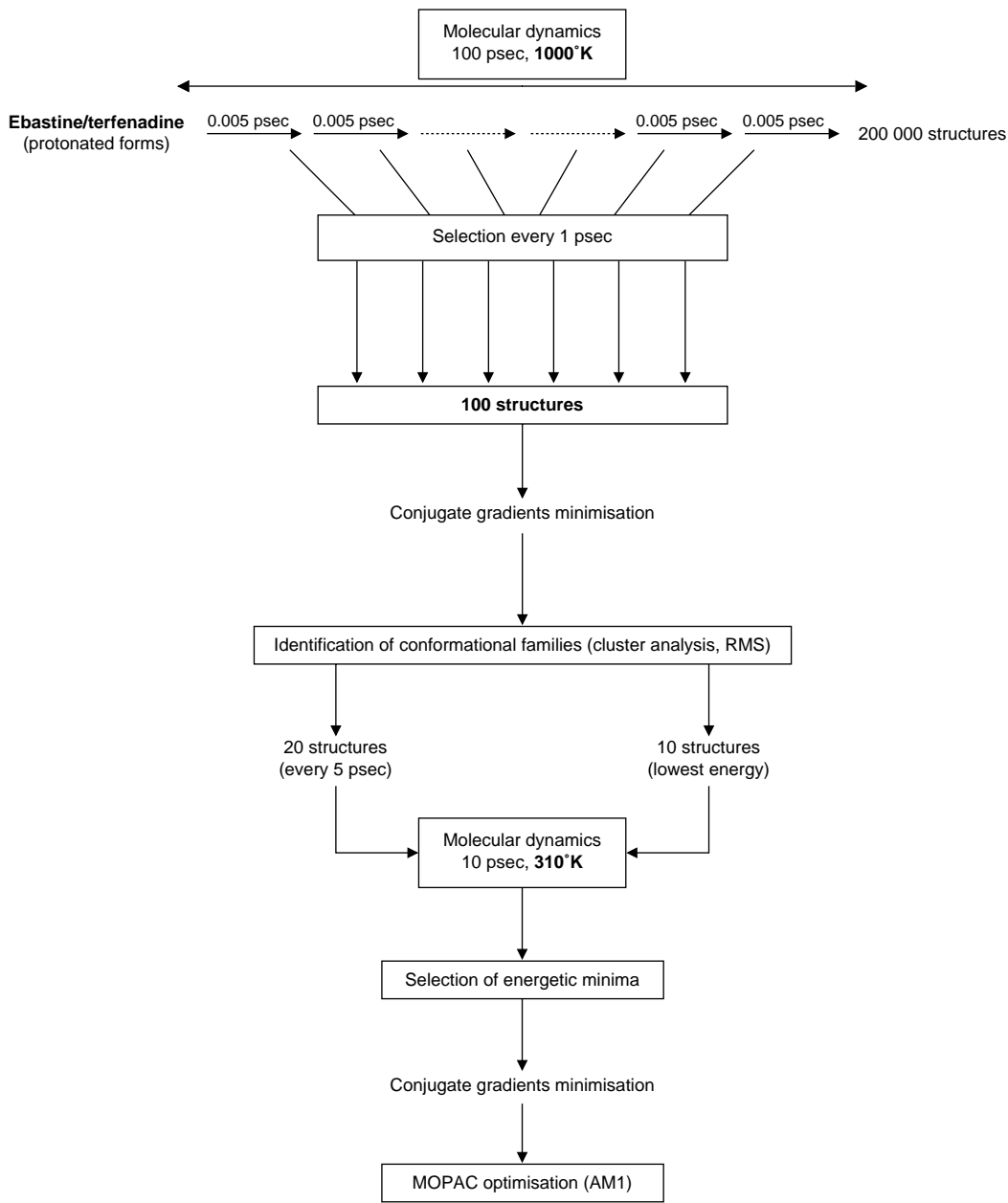


**Fig. 2.** Molecular dynamics protocol followed in the conformational search of ebastine and terfenadine. **MOPAC** = Molecular Orbital PACKage; **RMS** = root mean square.

temperature of 1000°K allows the molecule to adopt a number of conformations that are separated by barriers that would be crossed very infrequently at room temperature. This type of calculation provides a sample of conformations and their potential energies. Thus, the probability of finding one or more active conformations is heavily dependent on the conformational space explored. In order to assess the search effectiveness, both the cartesian space and the Van der Waals energy surface were analysed.

However, as suggested by the pKa values, terfenadine<sup>[36]</sup> and ebastine ( $10.32 \pm 0.51$ , calculated by the solubility method described by Albert and Serjeant<sup>[37]</sup>) have a protonatable nitrogen at physiological pH. It is likely, therefore, that most of their interactions with biological targets will take place in the ionised form, as happens with the H<sub>1</sub> receptor (interaction with Asp<sub>116</sub> residue).<sup>[38]</sup> For this reason, the behaviours of terfenadine and ebastine have been studied in the protonated forms.

#### **Conformational Space of Ebastine**

**N-equatorial protonated form:** With an eq-Neq conformation as the starting point, and after a molecular dynamics procedure at 1000°K followed by analysis of selected structures every 5 psec, ebastine preferred to adopt eq-Neq chair piperidine ring conformations (65%) along the trajectory, whereas only 11% show an ax-Nax arrangement. Molecular dynamics simulation at 310°K of selected structures yields 4 different geometries (fig. 3: 1a-1d): two with extended disposition, either eq-Neq (1a) or changing the chair form ax-Nax (1b), and the other two stabilised by an intramolecular hydrogen bond: 1c (ax-Nax) and 1d (eq-Neq). The most abundant conformations in the molecular dynamics simulation were not the most stable ones after AM1 optimisation.

**N-axial protonated form:** A different behaviour can be observed in the simulation starting from the eq-Nax conformation. In this instance, molecular dynamics simulation at 1000°K reveals that the diphenyl methoxy substituent prefers to adopt an axial (52%) rather than an equatorial (13%) orientation. After analysis of the selected conformations,

molecular dynamics simulation at 310°K gives 4 families of conformations, as shown in figure 3 (1e-1h). Once again, the inversion of the piperidine chair takes place, and the ax-Neq and eq-Nax dispositions can be identified. Two conformations are stabilised by an intramolecular hydrogen bond (1e, ax-Neq, and 1f, eq-Nax), and two show an extended arrangement (1g, eq-Nax, and 1h, ax-Neq).

#### **Conformational Space of Terfenadine**

**N-equatorial protonated form:** Along the trajectory, in the 1000°K simulation, terfenadine displays 93% of all-equatorial conformation, as against 2% of all-axial disposition. Molecular dynamics simulation at 310°K of different conformations belonging to each family yields 4 structures (fig. 4): two compounds with an eq-eq conformation of the piperidine ring chair (2a-2b), and two others with an axial-axial arrangement of the piperidine ring chair (2c-2d). The conformers 2b and 2d are stabilised by an intramolecular hydrogen bond. This second group of conformations represents isolated energy minima (more stable but less abundant in comparison with the 1000°K and 310°K simulation).

**N-axial protonated form:** High temperature molecular dynamics simulation (1000°K) shows that structures have a tendency to be distributed into 3 classes of conformations: two piperidine ring chair families, eq-Nax (19%) and ax-Neq (8%), and the transitional eq-eq twisted-boat and boat arrangements (73%). As can be seen, the high number of boat transitional conformations show that terfenadine prefers to be in an all-equatorial arrangement, even at the expense of avoiding chair conformations. A similar profile was obtained after simulation of different families at 310°K. The most stable and abundant conformations are represented in figure 4 (2e-2h). The conformation 2e has the lowest energy, but appears only for 3 to 4 psec of the whole simulation, indicating that there is a low probability of its being obtained. On the contrary, the twisted-boat conformation 2f can be found in abundance, with an energy difference compared with 2e of  $2.6 \text{ kcal} \cdot \text{mol}^{-1}$ . The rest of the conformers, 2g and 2h, differ only in the piperidine

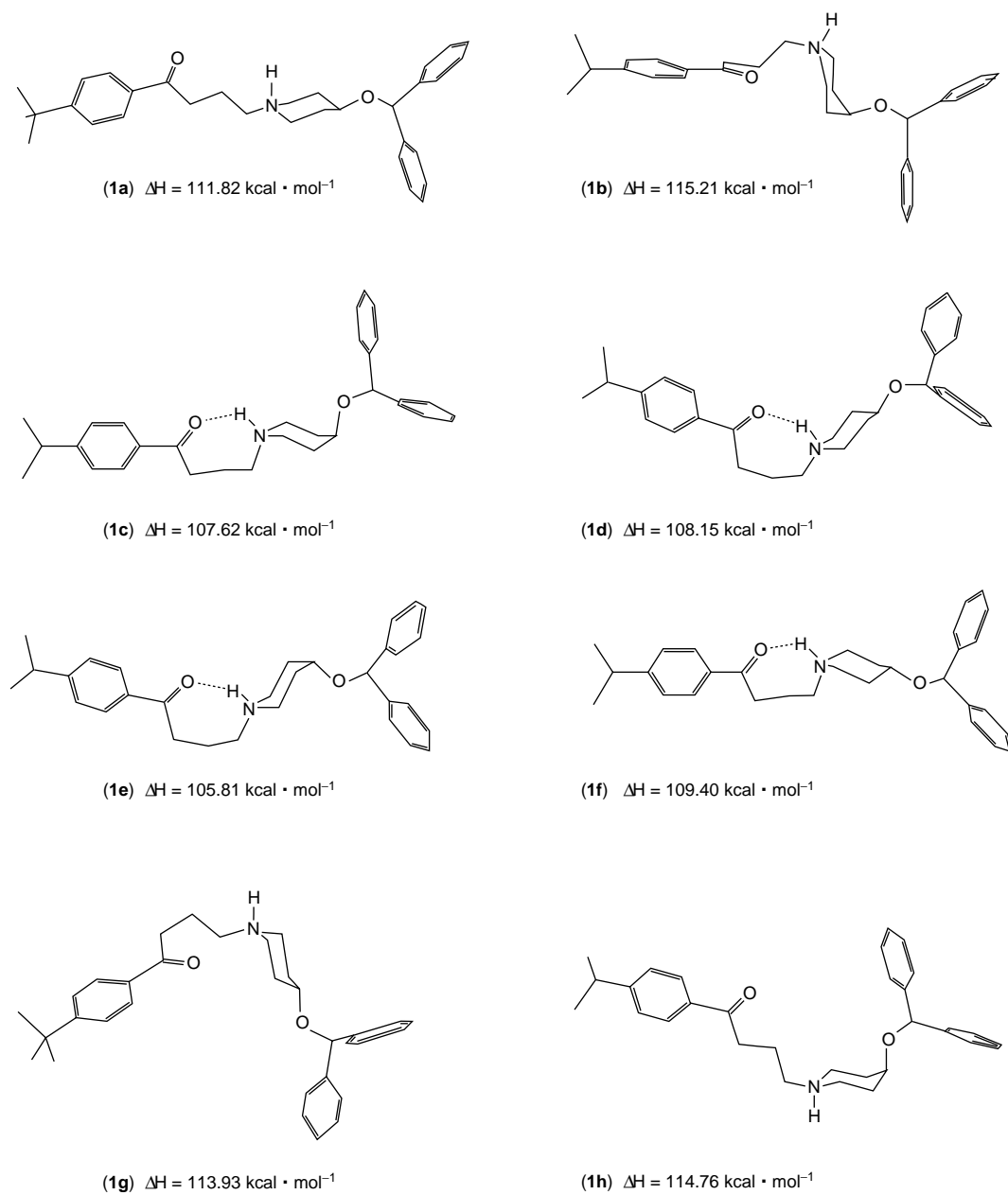


**Fig. 3.** Preferred conformations obtained from the dynamics simulation of the protonated forms of ebastine.

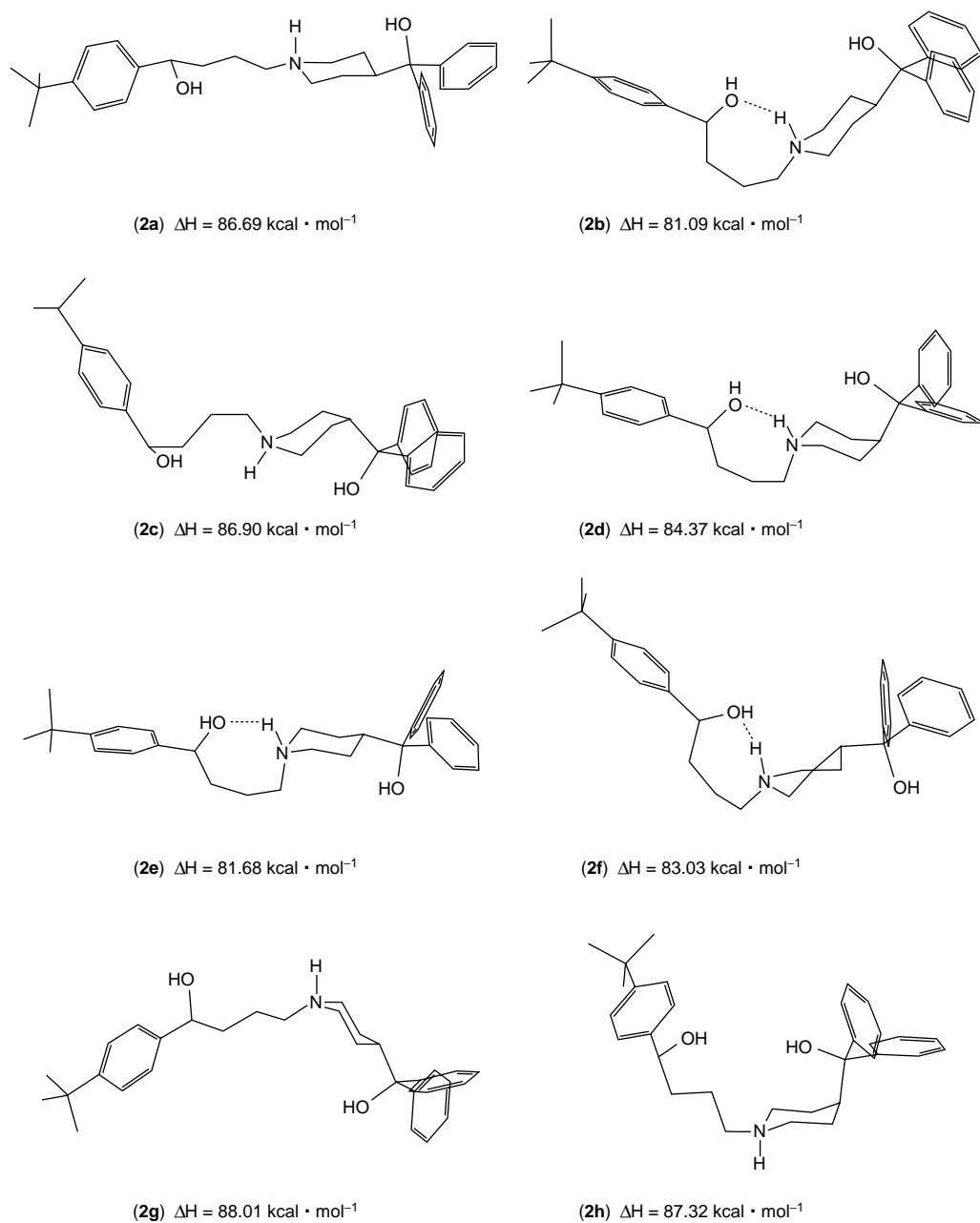


**Fig. 4.** Preferred conformations obtained from the dynamics simulation of the protonated forms of terfenadine.

chair conformation, with the chain remaining in an extended arrangement.

### Selection of Conformations

For the following studies, we deliberately selected from the most representative conformations those that were most similar in the two compounds, despite the clearly different conformational behaviour of ebastine and terfenadine, which will be addressed in a later section.

Two different types of conformations were selected: an extended disposition, with an eq-Neq arrangement (conformation 1a for ebastine and 2a for terfenadine), and a folded disposition showing stabilisation by intramolecular hydrogen bonds, in this instance with an eq-Nax arrangement (conformation 1f for ebastine, and 2e for terfenadine).

Table I shows the distances between heteroatoms and centroids of phenyl rings for selected

conformations of ebastine and terfenadine, respectively.

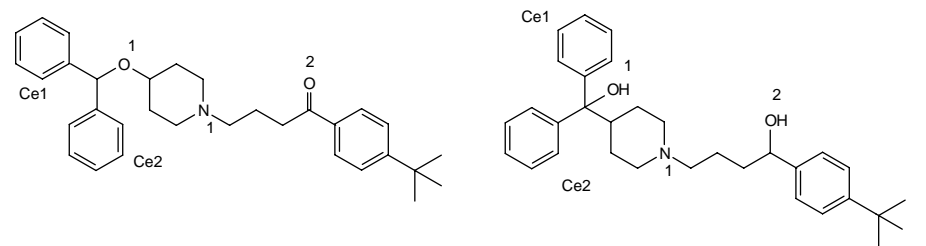
### Electronic Properties Derived from Quantum Mechanics

#### Molecular Electrostatic Potentials

The positive charge of the ammonium cation shifts the negative electrostatic potential surfaces towards positive energy values. Therefore, all the MEP maps of the protonated forms that show the equivalent of negative interactions have been represented at 15 kcal (fig. 5).

In the fully extended conformation (1a), ebastine exhibits 3 well-defined electrostatic interaction regions, two located in the neighbourhood of the phenyl rings and the third one situated around the lone pairs of the oxygen atom in the carbonyl group. By contrast, terfenadine in its equatorial-equatorial extended conformation (2a) exhibits

**Table I.** Distances in angstrom units between heteroatoms and the centroids of phenyl rings of selected ebastine and terfenadine conformations after AM1 optimisation (Molecular Orbital PACKage)



Distances	Ebastine conformations		Terfenadine conformations	
	1a	1f	2a	2e
N1-O1	4.2099	4.1800	4.4983	4.4736
O1-O2	7.0665	8.7927	8.9462	7.0516
O2-N1	2.8673	5.0787	5.1243	2.8598
Ce1-O1	3.6761	3.6818	3.6341	3.6729
Ce1-N1	6.6708	6.6677	6.2640	6.3661
Ce1-O2	9.2650	11.5269	9.7730	9.0495
Ce2-O1	3.6045	3.6018	3.6815	3.6695
Ce2-N1	7.6857	7.6525	6.4512	6.3222
Ce2-O2	10.4880	11.7507	11.4158	8.1365
Ce2-Ce1	4.8209	4.8091	4.7158	4.8138



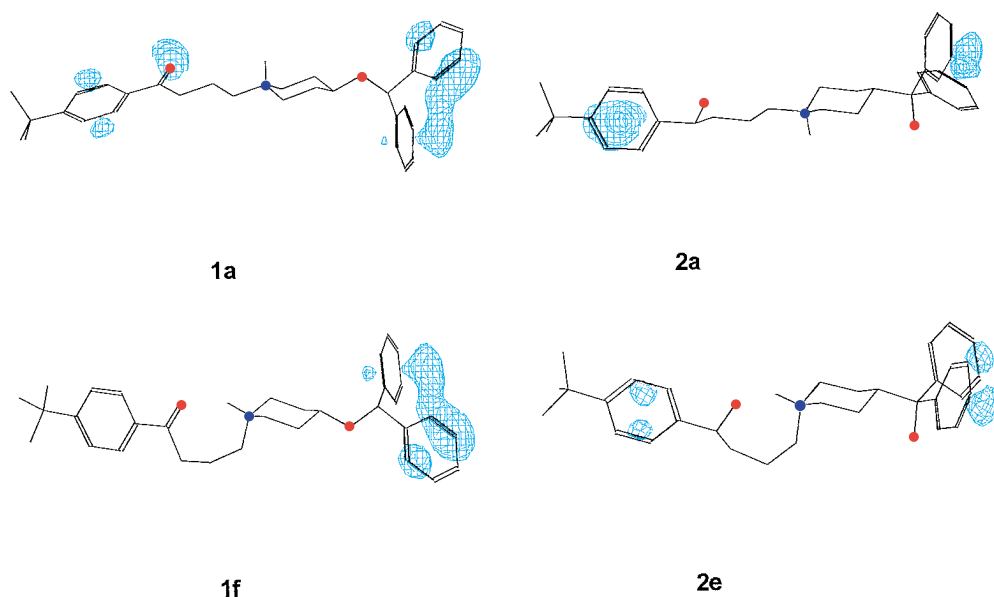


**Fig. 5.** Molecular electrostatic potential maps of selected protonated conformations of ebastine (1a,1f) and terfenadine (2a,2e). Maps are contoured at 15 kcal • mol.

only 2 interaction areas because of the lack of electrostatic potential over the hydroxy group at the represented level.

For both folded N-axial conformations, probably because of the formation of an intramolecular hydrogen bond, neither ebastine (conformation 1f) nor terfenadine (conformation 2e) exhibited electrostatic potential areas around the heteroatoms. For these conformations, the only interactions found were in the regions around the phenyl rings.

#### **Frontier Orbitals (HOMO, LUMO)**

The protonation of the basic nitrogen changes the situation of the frontier orbitals with respect to the neutral forms. As depicted in figure 6, the positive charge on the nitrogen atom produces a loss of electronic density, and the LUMO is situated around the piperidine moiety in both compounds. On the contrary, the electron withdrawing effect of the carbonyl group of ebastine (conformations 1f and 1a) shifts the HOMO towards the diphenyl

fragment, whereas in terfenadine (conformations 2a and 2e) it remains on the tert-butylphenyl group. The energy values of the frontier orbitals are quantified in table II.

#### **Interaction Maps Derived from GRID Calculations**

In many instances, possible energetically favourable binding sites in the ligands can be identified by determining which type of binding forces can be accomplished with the receptor site. For this purpose, we calculated several GRID maps for the selected conformers with the aim of determining the similarities and/or differences in their binding sites. Three different probes were chosen: i) a neutral flat NH amide (probe N1) to describe the hydrogen bond acceptor regions in the molecule; ii) an  $sp^2$  carbonyl oxygen (probe O) to locate the hydrogen bond donor regions; and iii) an ionised alkyl carboxy group (probe  $COO^-$ ) to calculate

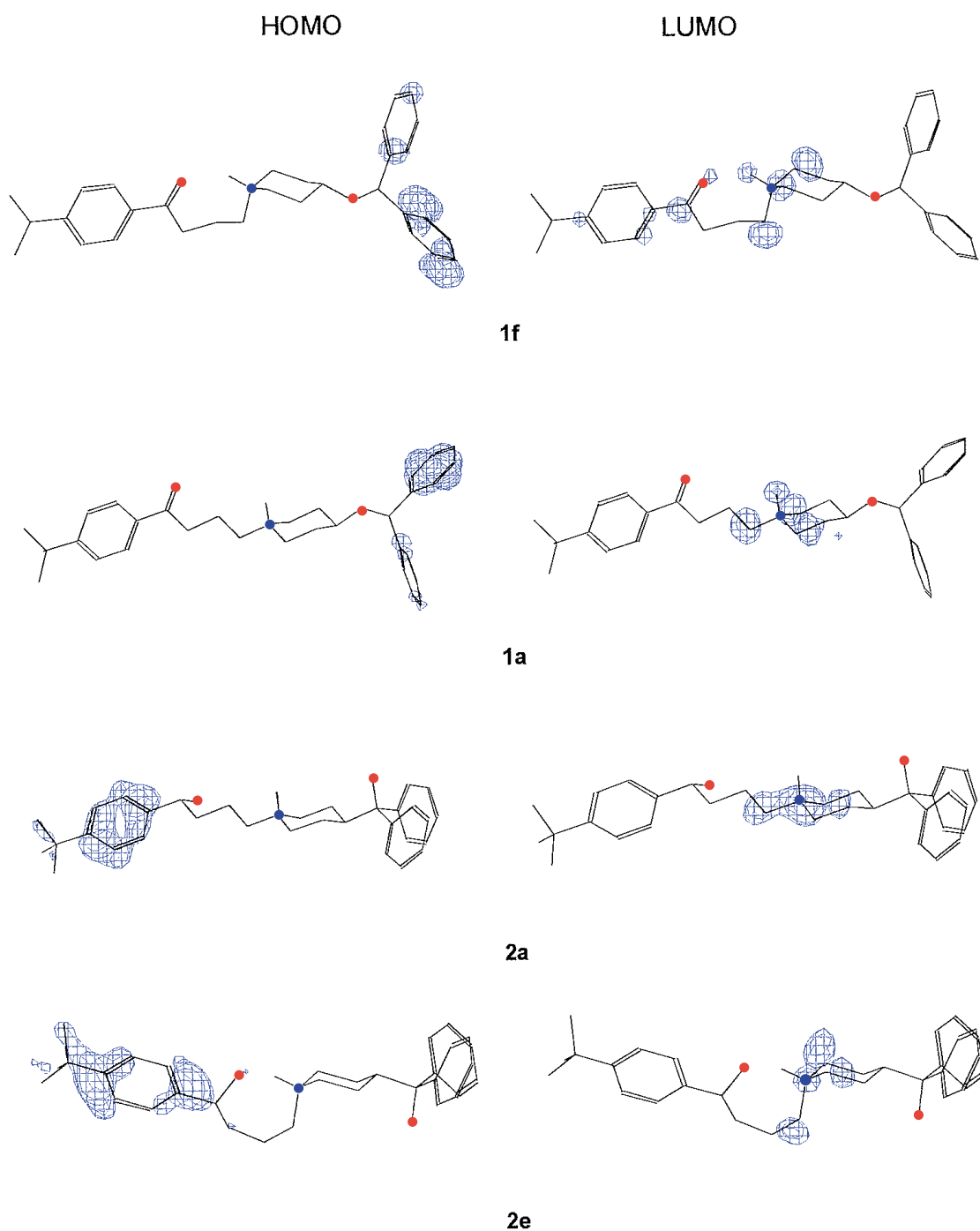


**Fig. 6.** Distribution of frontier orbitals, the highest occupied molecular orbital (HOMO) and the lowest unoccupied molecular orbital (LUMO), in the selected protonated conformations of ebastine (1a, 1f) and terfenadine (2a, 2e). Maps are contoured at 0.05 electron/Å<sup>3</sup>.

**Table II.** HOMO-LUMO coefficients in several fragments of the selected protonated forms of ebastine (1f and 1a) and terfenadine (2a and 2e)

Compounds	Selected fragments					
	tert-butylphenyl		piperidine		diphenylmethyl	
	$\xi_{\text{HOMO}}$ (eV) <sup>a</sup>	$\xi_{\text{LUMO}}$ (eV)	$\xi_{\text{HOMO}}$ (eV)	$\xi_{\text{LUMO}}$ (eV)	$\xi_{\text{HOMO}}$ (eV)	$\xi_{\text{LUMO}}$ (eV)
1f	<10 <sup>-6</sup>	<10 <sup>-6</sup>	0.0076	1.59	7.80	<10 <sup>-6</sup>
1a	<10 <sup>-6</sup>	0.3	0.007	1.61	10.83	<10 <sup>-6</sup>
2a	9.96	0.004	0.009	2.15	<10 <sup>-6</sup>	<10 <sup>-6</sup>
2e	10.22	0.0026	<10 <sup>-6</sup>	1.6	<10 <sup>-6</sup>	<10 <sup>-6</sup>

<sup>a</sup> 1 eV =  $1.6 \times 10^{-12}$  J.

**HOMO** = highest occupied molecular orbitals; **LUMO** = lowest unoccupied molecular orbitals.

possible interactions with an acidic residue. This last probe was selected following previous work by Ter Laak and co-workers,<sup>[38]</sup> who describe an aspartate residue (Asp<sub>116</sub>) coupled to the protonated amino group of the molecule.

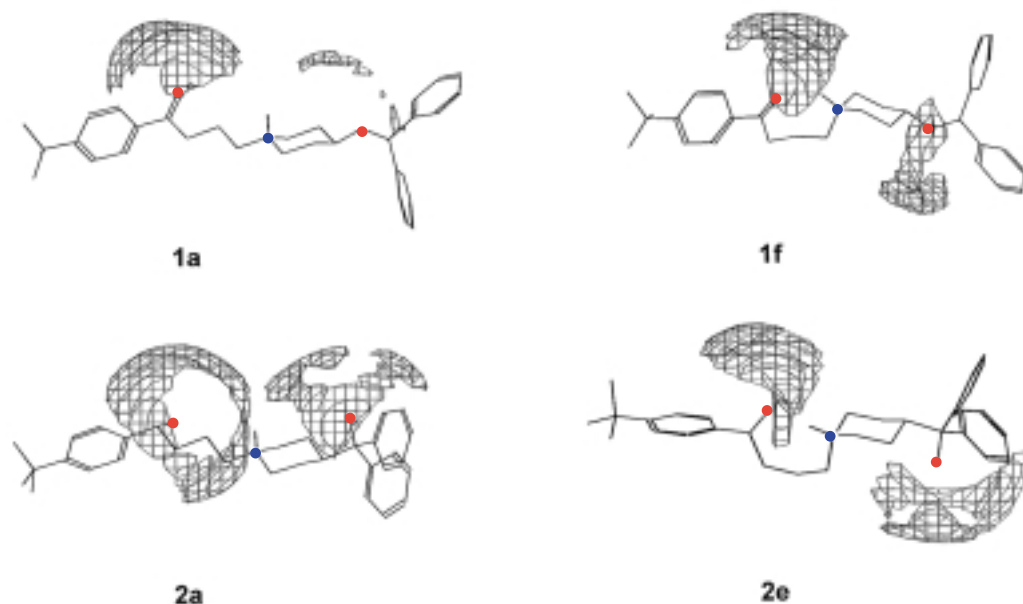
#### N1 Probe

Figure 7 depicts the interaction maps of protonated conformations of ebastine (1a and 1f) and terfenadine (2a and 2e) obtained with the N1 probe (neutral flat NH amide), contoured at the level of  $-4 \text{ kcal} \cdot \text{mol}^{-1}$ . For both compounds, two areas of interaction can be observed, although these are

more intense for terfenadine. Depending on the conformation, the areas of interaction may be placed in different relative positions.

#### O Probe

The interaction regions obtained for protonated ebastine and terfenadine with the O probe ( $\text{sp}^2$  carbonyl oxygen) at the level of  $-3 \text{ kcal} \cdot \text{mol}^{-1}$  are shown in figure 8. For ebastine, only a small area of interaction is found for the fully extended conformation (1a) corresponding to the protonated nitrogen. This area almost disappears in the folded conformation (1f), in which the protonated

**Fig. 7.** Interaction regions of protonated ebastine (1a,1f) and terfenadine (2a,2e) obtained with the N1 probe.

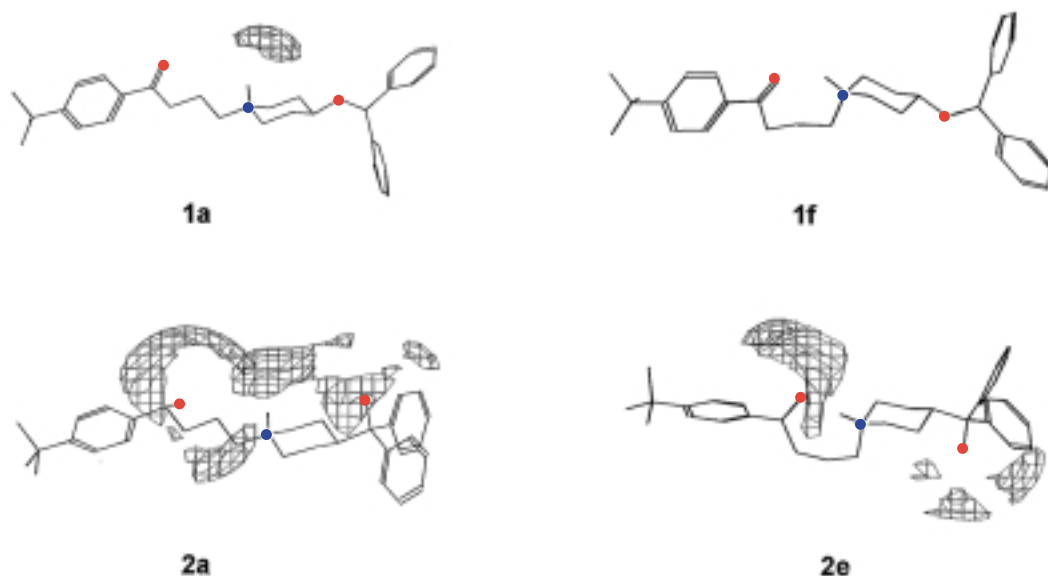


Fig. 8. Interaction regions of protonated ebastine (1a,1f) and terfenadine (2a,2e) obtained with the O probe.

nitrogen forms an intramolecular hydrogen bond. By contrast, in the maps obtained for terfenadine, several additional large areas of interaction associated with the hydroxyl groups are found.

#### COO<sup>-</sup> Probe

The interaction maps (fig. 9) with the COO<sup>-</sup> multi-atom probe (ionised alkyl carboxy group) for ebastine and terfenadine are quite similar, and the most important variation is observed in the type of conformation. Thus, in the fully extended conformations (1a, 2a), the main area of interaction is obviously located around the positively charged nitrogen, while in the folded conformations this interaction is clearly reduced. In this instance, if H<sub>1</sub> receptor antagonism does require the protonated nitrogen to be coupled with an aspartate residue in the binding site,<sup>[38]</sup> an extended conformation without an intramolecular hydrogen bond is the most likely bioactive conformation for both compounds.

#### Study of GRID Maps in Related Compounds

Figure 10 shows the interaction GRID maps of several related compounds with the carbonyl

oxygen probe. Cetirizine and chlorpheniramine demonstrate interaction only in the protonated nitrogen area, while haloperidol, astemizole and cisapride show additional areas of interaction.

## Discussion

### Conformational Space

The conformational behaviour of ebastine and terfenadine has been studied by molecular dynamics techniques.

Both N-axial and N-equatorial arrangements were selected as starting points for the molecular dynamics simulations. From the N-equatorial protonated disposition, both eq-Neq and ax-Nax arrangements, in either extended or folded shapes stabilised by intramolecular hydrogen bonds, are found for both ebastine and terfenadine. However, the number of conformations found with intramolecular hydrogen bonds is much higher for ebastine.

In the N-axial protonated forms, terfenadine behaves in a peculiar fashion in that it appears as if neither an eq-Nax nor an ax-Neq arrangement is comfortable for it. Thus, during the dynamics tra-

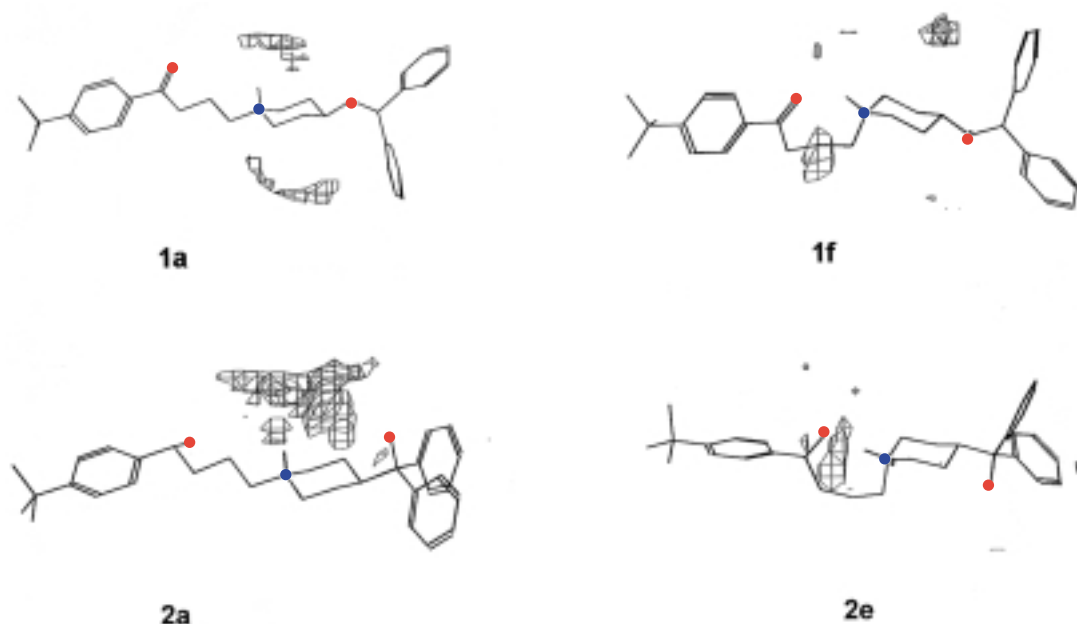


Fig. 9. Interaction regions of protonated ebastine (1a,1f) and terfenadine (2a,2e) obtained with the COO<sup>-</sup> probe.

jectory, most of the conformations prefer to adopt transitional shapes, such as boats and twisted-boats, thereby orientating the substituents into equatorial disposition. Some of these transition conformations were selected for the low temperature molecular dynamics simulation, in which twisted-boat conformers stabilised by intramolecular hydrogen bonds were obtained. After quantum mechanics optimisation, they became very stable. In the case of ebastine, the N-ax simulation yields 4 types of stable and abundant conformations: eq-Nax and ax-Neq, either in extended or folded hydrogen bond stabilised conformations.

Ebastine therefore exhibits a high framework flexibility because of abundant eq-Nax, ax-Neq and ax-Nax conformations found along the whole dynamics trajectory. By contrast, terfenadine exhibits some conformational restrictions in terms of the dynamics population. This means that eq-Nax protonated forms prefer to adopt twisted-boat conformations orientating their substituents equatorially, rather than piperidine chair conformations

with axial substituents, clearly demonstrating a different conformational behaviour in comparison with ebastine.

#### Molecular Electrostatic Potential

Electrostatic interaction has been shown to be a critical component of the intermolecular interaction in many biological processes, and MEPs have been found to provide a useful insight into the differential biological activity within chemical families.<sup>[39-41]</sup>

The MEP maps calculated for protonated conformations show that the level of interaction of the carbonylic oxygen in ebastine is higher than that observed for the corresponding hydroxyl group in terfenadine. In fact, at the contour level studied, fully extended ebastine exhibits 3 interaction points, whereas terfenadine exhibits only 2, with the diphenyl aromatic regions common to both compounds.

## Frontier Orbitals

Among the electronic properties, the nature and energy of the HOMOs and LUMOs are related to the ability of the molecule as a whole, and of regions in particular, to be involved in an electron transfer interaction with a target macromolecule.<sup>[42,43]</sup>

Molecular orbital calculations indicate that, in terms of electron transfer interaction, ebastine and terfenadine behave very differently. The LUMO orbital is located on the piperidine ring for both compounds, whereas the HOMO orbital is found around the tert-butylphenyl group of terfenadine and, in ebastine, at the opposite end of the molecule, around the diphenylmethyl moiety. No differences were found between different types of conformations.

Regarding antihistamine activity, a comparative study with several classical histamine H<sub>1</sub> antagonists has shown a lack of correlation between LUMO energy and activity,<sup>[44]</sup> and the different shapes and distributions of the frontier orbitals were dependent on the antihistaminic chemical moiety.

## GRID Maps

In this study, the areas of interaction between the molecules and the different atom and multi-atom probes, which give detailed information about possible binding sites, have been mapped in 3-dimensional space by use of the program GRID. A neutral flat NH amide and an sp<sup>2</sup> carbonyl oxygen were respectively used as probes for hydrogen bond acceptor regions and hydrogen bond donor regions in the molecule. Additionally, an ionised alkyl carboxy group was employed to calculate possible interactions with an acidic residue, such as that described previously.

Both ebastine and terfenadine have areas of interaction where the NH amide probe may interact, either with the hydroxyl groups of terfenadine or with the carbonyl and ether functions in ebastine. The position of these areas of interaction depends on the conformation.

As demonstrated in the Results section, the areas of interaction obtained with the multi-atom carboxy probe differ with the types of conformation studied (extended vs folded stabilised by an intramolecular hydrogen bond). If the interaction between the aspartate residue (Asp<sub>116</sub>) and the protonated amino group of the antagonist is essential for receptor-ligand association, then an extended conformation, without the formation of intramolecular hydrogen bonds, is the most likely bioactive conformation.

The interaction maps obtained with the carbonyl oxygen probe reveal a marked difference between ebastine and terfenadine. For ebastine, only a small area of interaction is observed, corresponding to the protonated nitrogen. By contrast, the hydroxyl groups of terfenadine, which have been replaced by the carbonyl and ether groups in ebastine, are also able to produce hydrogen bond donor interactions, and two large additional areas of interaction are observed. These data are important because they are related to additional points of binding, which are clearly not relevant for the antihistamine H<sub>1</sub> activity, but which may play a role in other pharmacological activities, including those related to secondary adverse effects such as cardiotoxicity.

## Studies with Other Compounds

The preceding finding, in which additional areas of interaction as a hydrogen bond donor were found for terfenadine, prompted us to study several other compounds, including H<sub>1</sub> histamine antagonists (both with and without documented cardiotoxicity), as well as drugs used for noncardiac indications that had been documented as inducing adverse cardiac effects in clinical practice.

We selected astemizole, haloperidol and cisapride, all of which have been reported to be associated with prolongation of the QT interval and torsade de pointes in humans, and cetirizine and chlorpheniramine, antihistamine drugs apparently free from arrhythmogenic effects.

Figure 10 shows the GRID maps for interaction of these selected compounds with the carbonyl oxygen probe. Structural comparison of haloperidol,

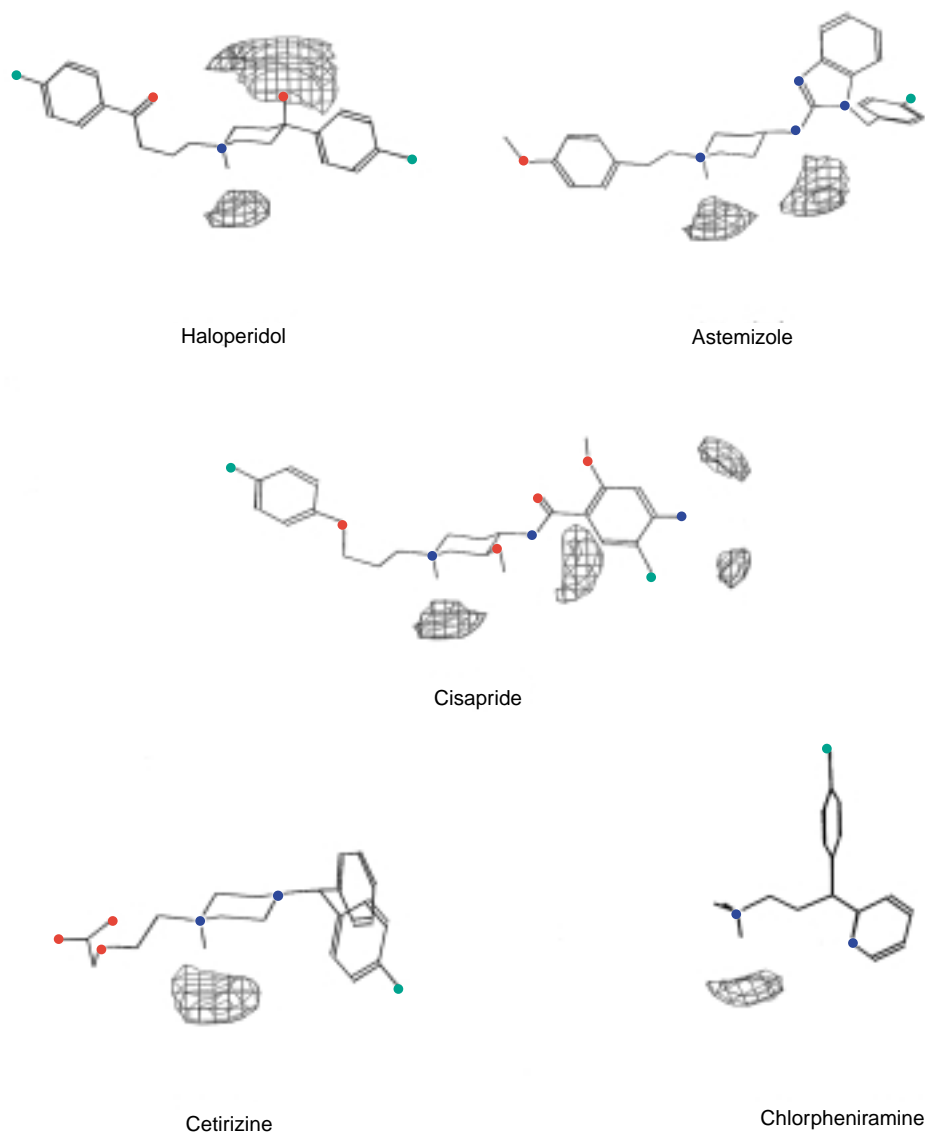


**Fig. 10.** Interaction GRID maps of other drugs with the carbonyl oxygen probe.

astemizole and cisapride shows that all these compounds exhibit a hydrogen bond donor group located between the phenyl or diphenylmethyl substituents and the basic nitrogen atom. The GRID maps also indicate the presence of at least one additional region of interaction, as seen with

terfenadine, generated by the hydroxy group in haloperidol and the NH group in astemizole and cisapride.

By contrast, the GRID maps of cetirizine and chlorpheniramine, like that of ebastine, exhibit only hydrogen bond donor interactions due to the

protonated nitrogen, and additional hydrogen bond donor areas, as seen with terfenadine, haloperidol, astemizole and cisapride, are absent.

Whether this apparent correlation between the ability to form additional hydrogen bond donor interactions and the induction of cardiac arrhythmias is simply coincidence or definitive cause and effect is open to debate, and obviously further studies are required to establish the real nature of the relationship of one phenomenon with the other.

## Conclusions

In conclusion, the use of molecular dynamics simulation to thoroughly explore conformational space in their protonated forms has shown that ebastine behaves differently from terfenadine.

The study of several quantum mechanics-based properties for the pairs of closest conformations in both compounds shows only that the MEP is slightly different. By contrast, the study of wave-function maps and distribution coefficients demonstrates very different allocations of HOMO orbitals in the protonated forms for ebastine compared with terfenadine.

Analysis of the putative interaction sites by means of the program GRID, and using a variety of probes, reveals clear additional hydrogen bond donor sites present in terfenadine but absent in ebastine.

Additional interaction sites are also present in astemizole, haloperidol and cisapride (other compounds known to prolong the QT interval and induce torsade de pointes), but are absent in chlorpheniramine and cetirizine (compounds not associated with arrhythmogenic effects). These findings suggest a possible cause-and-effect relationship between one phenomenon and the other, although clearly other factors such as lipophilicity must also be considered.

## References

- Moragues J, Roberts DJ. Ebastine. *Drugs Future* 1990; 15: 674-9
- Wiseman LR, Faulds D. Ebastine. A review of its pharmacological properties and clinical efficacy in the treatment of allergic disorders. *Drugs* 1996; 51: 260-77
- Van Drooge MJ, Donnéop den Kelder GM, Timmerman H. The histamine H<sub>1</sub>-receptor antagonist binding site. Pt I. Active conformation of cyproheptadine. *J Comput Aided Mol Des* 1991; 5: 357-70
- Ter Laak AM, Van Drooge MJ, Timmerman H, et al. QSAR and molecular modelling studies on histamine H<sub>1</sub>-receptor antagonists. *Quant Struct Act Relatsh* 1992; 11: 348-63
- Borea PA, Bertolasi V, Gilli G. Crystallographic and conformational studies on histamine H<sub>1</sub>-receptor antagonists. *Arzneimittel Forschung* 1986; 36: 895-9
- Sorkin EM, Heel RC. Terfenadine: a review of its pharmacodynamic properties and therapeutic efficacy. *Drugs* 1985; 29: 34-56
- Martínez-Tobed A, Tarrus E, Segura J, et al. Pharmacokinetic studies of ebastine in rats, dogs and man. *Drugs Today* 1992; 28 Suppl. B: 57-67
- Llupia J, Bou J, Fernández AG, et al. Antihistamine, anti-allergic and related pharmacological properties of ebastine, a new selective histamine H<sub>1</sub>-receptor antagonist. *Drugs Today* 1992; 28 Suppl. B: 11-21
- Roberts DJ. A preclinical overview of ebastine. Studies on the pharmacological properties of a novel histamine H<sub>1</sub> receptor antagonist. *Drugs* 1996; 52 Suppl. 1: 8-14
- Monahan BP, Ferguson CL, Killeavy ES, et al. Torsades de pointes occurring in association with terfenadine use. *JAMA* 1990; 264: 2788-90
- Woosley RL, Chen Y, Freiman JP, et al. Mechanism of the cardiotoxic actions of terfenadine. *JAMA* 1993; 269: 1532-6
- Crumb WJ, Wible B, Arnold DJ, et al. Blockade of multiple human cardiac potassium currents by the antihistamine terfenadine: possible mechanism for terfenadine-associated cardiotoxicity. *Mol Pharmacol* 1995; 47: 181
- Kii Y, Inui A, Ito T. Effects of histamine H<sub>1</sub> receptor antagonists on action potentials in guinea-pig isolated papillary muscles. *Arch Int Pharmacodyn Ther* 1996; 331: 59-73
- Yang T, Prakash C, Roden DM, et al. Mechanism of block of a human cardiac potassium channel by terfenadine racemate and enantiomers. *Br J Pharmacol* 1995; 115: 267-74
- Valenzuela C, Delpon E, Franqueza L, et al. Comparative effects of a non-sedating histamine H<sub>1</sub>-receptor antagonist on human Kv1.5 channels. *Br J Pharmacol* 1996; 118: 105P
- Gras J, Llenas J, Palacios JM. Ebastine is without effect in a sensitive experimental model for detecting prolongation of the QTc interval. *Allergy* 1996; 51 Suppl. 31: 188
- Hey JA, del Prado M, Sheerwood J, et al. Comparative analysis of the cardiotoxicity proclivities of second generation antihistamines in an experimental model predictive of adverse clinical ECG effects. *Arzneimittel Forschung* 1996; 46 (1): 153-8
- Roberts DJ, Llenas J. Second generation antihistamines and cardiotoxicity. *Arzneimittel Forschung* 1996; 46 (2): 832-4
- Hey JA, del Prado M, Kreutner W, et al. Cardiotoxic and drug interaction profile of the second generation antihistamines ebastine and terfenadine in an experimental animal model of torsade de pointes. *Arzneimittel Forschung* 1996; 46 (1): 159
- Gras J, Llenas J, Palacios JM, et al. The role of ketoconazole in the QTc interval prolonging effects of H<sub>1</sub>-antihistamines in a guinea-pig model of arrhythmogenicity. *Br J Pharmacol* 1996; 119: 187-8
- Williams A, Redfern WS, Day A, et al. Prolongation of the QTc interval by ketoconazole in conscious guinea-pigs implanted with ECG telemetry transducers. *Br J Pharmacol* 1996; 119: 356P
- ChemX version, Jan 1996. Oxfordshire, England: Chemical Design Limited, 1996
- Davies EK, Murrall NW. How accurate does a force field need to be? *Computers Chem* 1989; 13: 149-56



24. Ortiz AR, Pisabarro MT, Gago F. Molecular model of interaction of bee venom phospholipase A<sub>2</sub> with manolide. *J Med Chem* 1993; 36: 1866-79
25. Gordon HL, Somarjai RL. Fuzzy cluster analysis of molecular dynamics trajectories. *Proteins Struct Funct Genet* 1992; 14: 249-64
26. Shenkin PS, McDonald DQ. Cluster analysis of molecular conformations. *J Comput Chem* 1994; 15: 899
27. SAS Release 6.10. Cary, North Carolina: SAS Institute Inc, 1993
28. MOPAC/AM1 method of version 6.00 (Bloomington, IN, USA: Quantum Chemistry Program Exchange (QCPE), Program no. 506), 1990. Program VSS (QCPE, Program no. 249), 1974
29. Stewart J, James P. MOPAC: a semiempirical molecular orbital program. *J Comput Aided Mol Des* 1990; 4: 1-105
30. Giessner-Pretre C, Pullman A. Molecular electrostatic potentials. Comparison ab initio and CNDO (Complete neglected of differential overlap) results. *Theor Chim Acta (Berlin)* 1972; 25: 83-8
31. GRID version 14. Oxford, England: Molecular Discovery Limited, 1994
32. Goodford PJ. A computational procedure for determining energetically favorable binding sites on biologically important macromolecules. *J Med Chem* 1985; 28: 849-57
33. Wade RC, Clark KJ, Goodford PJ. Further development of hydrogen bond functions for use in determining energetically favorable binding sites on molecules of known structure. 1. Ligand probe groups with the ability to form two hydrogen bonds. *J Med Chem* 1993; 36: 140-7
34. Wade RC, Goodford PJ. Further development of hydrogen bond functions for use in determining energetically favorable binding sites on molecules of known structure. 2. Ligand probe groups with the ability to form more than two hydrogen bonds. *J Med Chem* 1993; 36: 148-56
35. Boobbyer DNA, Goodford PJ, McWhinnie PM, et al. New hydrogen bond potentials for use in determining energetically favorable binding sites on molecules of known structure. *J Med Chem* 1989; 32: 1083-94
36. Ter Laak AM, Tsai RS, Donn  op den Kelder GM, et al. Lipophilicity and hydrogen-bonding capacity of H<sub>1</sub>-antihistaminic agents in relation to their central sedative side-effects. *Eur J Pharm Sci* 1994; 2: 373-84
37. Albert A, Serjeant EP. The determination of ionization constants. London: Chapman and Hall Ltd, 1971
38. Ter Laak AM, Venhorst J, Donn  op den Kelder GM, et al. The histamine H<sub>1</sub>-receptor antagonist binding site. A stereoselective pharmacophoric model based upon (semi-)rigid H<sub>1</sub>-antagonists and including a known interaction site on the receptor. *J Med Chem* 1995; 38: 3351-60
39. Rabinowitz JR, Nambodiri K, Weinstein H. A finite expansion method for the calculation and interpretation of molecular electrostatic potentials. *Int J Quantum Chem* 1986; 29: 1697-704
40. Alkorta I, Villar HO. Molecular electrostatic potential of D1 and D2 dopamine agonists. *J Med Chem* 1994; 37: 210-3
41. Carrupt PA, El Tayar N, Karl  n A, et al. Molecular electrostatic potentials for characterizing drug-biosystem interactions. *Methods Enzymol* 1991; 203: 638-77
42. Loew GH, Villar HO, Alkorta I. Strategies for indirect computer-aided drug design. *Pharm Res* 1993; 10: 475-86
43. Szymoniak J, Boudon A, Chr  tien JR, et al. Drug design: LUMO control of neuroleptic pharmacophores [in French]. *Eur J Med Chem* 1987; 22: 101-7
44. Schweiger K, Weis R, Berthold H, et al. Computer assisted lead finding and optimization [abstract P-17.D]. Abstracts of the 11th European Symposium on Quantitative Structure Activity Relationships; 1996 Sep 1-6: Lausanne

---

Correspondence and reprints: Dr V. Segarra, Research Centre, Almirall Prodesfarma S.A., Cardener, 68-74, 08024 Barcelona, Spain.